Depletion of RAD17 sensitizes pancreatic cancer cells to gemcitabine

Johannes Fredebohm, Jonas Wolf, Jörg D. Hoheisel* and Michael Boettcher

Functional Genome Analysis, Deutsches Krebsforschungszentrum, Im Neuenheimer Feld 580, 69120 Heidelberg, Germany

*Author for correspondence (j.hoheisel@dkfz.de)

Accepted 24 April 2013
Journal of Cell Science 126, 3380–3389

doi: 10.1242/jcs.124768

Summary

Chemotherapy of advanced pancreatic cancer has mainly been gemcitabine-based for the past 15 years, with only limited effect. Recently, combination therapy that also targets checkpoint kinase 1 (CHK1) has become an attractive option. The central role of CHK1 in many DNA-damage response pathways, however, may result in undesired cytotoxicity in normal cells, causing side effects. We were searching for other target molecules of similar function that may be more specific and thus better suited for combination therapy. To this end a negative selection RNAi screen was performed in cell lines with small hairpin RNA molecules targeting over 10,000 genes. Genes that were found to be synthetically lethal with gemcitabine and whose proteins act upstream of CHK1 were characterised in more detail. In particular, the inhibition of RAD17 potentiated gemcitabine cytotoxicity in the pancreatic cancer cell lines BxPC-3 and MiaPaca-2 and in the primary cell line JoPaca-1 that closely resembles primary tumour tissue. Further analysis showed that the synergistic effect of RAD17 knockdown and gemcitabine leads to forced mitotic entry of cells arrested in S phase by gemcitabine treatment, resulting in asymmetric DNA distribution during anaphase followed by DNA fragmentation and finally cell death by mitotic catastrophe. Our data suggest RAD17 as a novel target protein for gemcitabine combination therapy supplementing or complementing inhibition of CHK1. In contrast to CHK1, RAD17 knockdown by itself does not lead to abnormal DNA segregation, suggesting a more specific action.

Key words: ATR/CHK1 signalling pathway, RAD17, Gemcitabine, Gemcitabine-combination therapy, Pancreatic cancer, shRNA screening

Introduction

Pancreatic cancer is a devastating disease. With a mortality rate that is almost identical to incidence and a five-year survival rate of less than 6%, it accounts for the fourth most common form of cancer-related deaths in the developed world (Siegel et al., 2013). Reasons for its poor prognosis are late diagnosis, highly invasive and metastatic potential and resistance to chemotherapeutics (Hung et al., 2012). Pancreatic ductal adenocarcinoma (PDAC) is the most common form of pancreatic cancer. The only potentially curative therapy is resection of the primary tumour followed by chemotherapy to try to eliminate residual tumour cells and metastases. At the time of diagnosis only about 20% of patients undergo tumour resection (Kern et al., 2011). The majority is diagnosed at an advanced stage of disease, with local invasion and distant metastases being present, which precludes surgery. Adjuvant chemotherapy with gemcitabine (GEM), the standard treatment for the last 15 years (Wang et al., 2011), can extend five-year survival to 25% in some cases (Hackert et al., 2009). In the last decade, gemcitabine has also been the standard in first-line treatment of non-resectable tumours. However, the clinical effect of gemcitabine monotherapy remains limited, with a response rate below 20% (Glienke et al., 2012).

Many clinical studies have tried to improve gemcitabine treatment by combining it with classical chemotherapeutics. However, clinical benefit for advanced PDAC has been limited so far (Merl et al., 2010; Stathis and Moore, 2010). A meta-analysis of 15 clinical trials looking at overall survival revealed that only patients with a good performance status could benefit from combinations of gemcitabine with platinum analogues or fluoropyrimidines (Heinemann et al., 2008). Likewise, combinations with targeted drugs have yielded only marginal effects. These include small molecules and therapeutic antibodies targeted against the extracellular receptors EGFR, VEGF or HER2, which are overexpressed in pancreatic cancer. Although when combined with bevacizumab (targeting VEGF) or trastuzumab (targeting HER2) there was no clinical benefit over gemcitabine alone (Ko et al., 2012; Safran et al., 2004), a small but significant 2-week improvement was observed when combined with the tyrosine kinase inhibitor erlotinib in patients with advanced PDAC (Moore et al., 2007). Overall, the rationale for gemcitabine combination therapies has been motivated by empirical data from other cancer entities in combination with end-point expressional data (Philip, 2008).

Over the past few years, advances in functional RNAi screening technologies have caused a paradigm shift in the field of target discovery (Iorns et al., 2007; Kassner, 2008). Rather than looking at gene expression changes from an end-point perspective, the functional approach addresses the whole process of drug-induced cytotoxicity. Thus, it is much more suitable for discovery of targets available for potential combination therapy. Following this principle, we conducted a synthetic lethal RNAi screen to identify new targets that – when depleted by RNAi – sensitize pancreatic cancer cells to gemcitabine.

Methodologically, two modules of the barcoded Decipher small hairpin RNA (shRNA) library were screened. Each module comprised 27,500 shRNA expression constructs targeting over 5,000 genes, with at least five constructs per gene. Using stringent filter criteria during analysis and validation, we

Journal of Cell Science

identified knockdown of the cell cycle checkpoint protein RAD17 homolog (from *Schizosaccharomyces pombe*; RAD17) to act in a synthetically lethal manner with gemcitabine in the cell lines BxPC-3, MiaPaca-2 and primary JoPaca-1 cells. RAD17 is involved in detecting gemcitabine-induced stalled replication forks and acts upstream of checkpoint kinase 1 (CHK1). Knockdown and inhibition of CHK1 has been shown to act in a synthetically lethal manner with gemcitabine in pancreatic cancer cells (Azorsa et al., 2009; Venkatesha et al., 2012), which was also confirmed in this study. Mechanistically, RAD17 in complex with replication factor C (RFC) subunits 2–5 is responsible for loading a DNA clamp composed of RAD9, RAD1 and HUS1 at stalled replication forks, a result of gemcitabine-induced masked chain termination. This early event in detection of stalled replication forks mediates activation of ataxia telangiectasia and Rad3 related (ATR) kinase, which is essential for downstream signalling, leading to cell cycle arrests. Our results show that the synergistic effect of RAD17 knockdown and gemcitabine is driven by forced mitotic entry of cells in which gemcitabine-induced stalled replication forks remain undetected. This leads to asymmetric DNA distribution during anaphase followed by DNA fragmentation and finally cell death by mitotic catastrophe.

Results

A negative selection RNAi screen was performed in BxPC-3 cells, targeting over 10,000 genes. The individual shRNA expression constructs were transduced into the cells by means of lentiviral infection. Negative selection pressure was induced by growing the cells with 6 nM gemcitabine (IC20) for 72 hours. Cytotoxic effects throughout the screen were monitored by quantification of the shRNA expression constructs through the associated barcode sequences. First, baseline cell viability for each shRNA expression construct was determined by detecting the barcode abundance prior to treatment (timepoint t_0). Second, synthetic lethality was calculated by dividing normalized barcode abundance of the treatment end point ($t_{\text{end-GEM}}$) by the control end point ($t_{\text{end-CTRL}}$) yielding a synthetic lethality (SL) ratio. Average SL ratios were calculated for a minimum of three independent shRNA expression constructs against the same gene. These synthetic lethal interactions were ranked by strength and significance determined by *t*-test comparison to internal negative control shRNAs against luciferase (Fig. 1). In total, there were 70 potential candidate genes with an average SL ratio significantly below a $\log_2$ of −0.35. Of all potential candidates, knockdown of RAD17 showed the most significant synthetic lethal effect (Fig. 1). The complete lists are shown in supplementary material Tables S1 and S2.

Prominent factors in DNA damage response validate screening procedure

To assess the quality of the screening procedure, we analysed the screening data for potential candidates by GO-annotation cluster enrichment analysis (Huang et al., 2009). We found that the most significantly enriched GO-annotation clusters contained genes involved in DNA damage and DNA repair signalling (Table 1). Candidate genes of these clusters were selected for validation. In response to gemcitabine-induced replication fork stalling, checkpoint kinase 1 (CHK1) plays a key role in downstream signalling in the ATR–CHK1 pathway. Among the selected candidates, four other proteins are directly involved in this signalling pathway, namely RAD17, HUS1, WEE1 and RCF3 (see Fig. 2B for an overview).

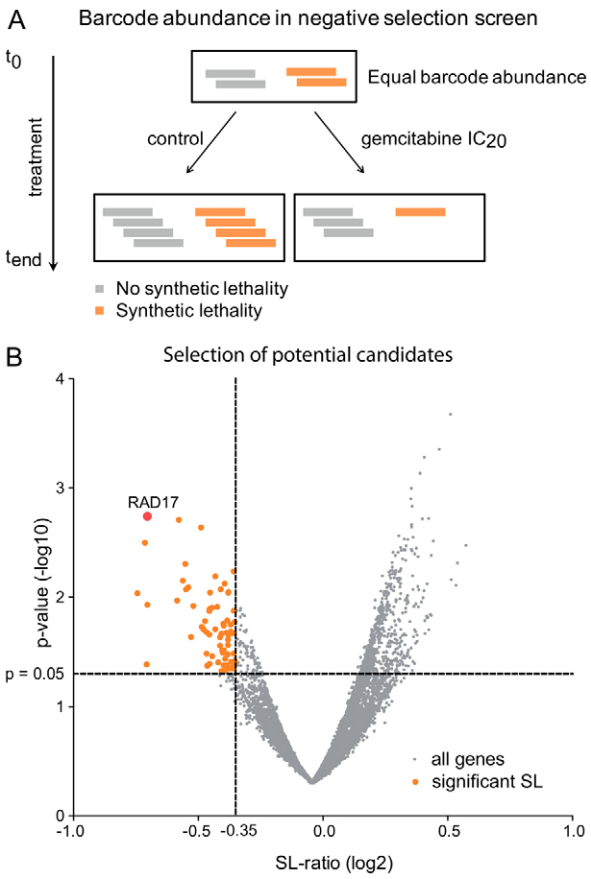

Fig. 1. Barcode abundance and selection of candidate genes. (**A**) The principle of barcode quantification for a negative selection screen is shown. Negative selection pressure induced by IC_{20} gemcitabine leads to increased barcode reduction of a synthetically lethal (SL) candidate (orange). Barcodes of shRNAs with no synthetic lethal effect (grey) are reduced in number by the treatment alone. (**B**) The actual screening results are presented, ranked by SL ratio and significance. Genes showing significant ($P<0.05$) SL ratios below −0.35 ($\log_2$) were selected for validation. RAD17 was most significant with an SL ratio of −0.704 ($\log_2$).

RAD17 and *CHK1* showed the strongest synthetic lethal effect in individual validation

Potential candidate genes were analysed individually for targeted gene knockdown using three independent shRNA expression constructs. As inhibition and knockdown of CHK1 is known to potentiate gemcitabine toxicity, shRNAs targeting *CHK1* were used as a positive control. Genes for which all three shRNA expression constructs showed synthetic lethality were *RAD17*, *WEE1* and *HUS1*, with a relative cell viability below 75%. The constructs affecting *RFC3* did not result in a significant reduction of viability (Fig. 2A). The strongest effect was observed for the knockdown of *RAD17*, which reduced relative viability below 75% for all three and below 50% for two constructs. Therefore, we focused on *RAD17* for further validation and characterization experiments. Depletion of RAD17 and CHK1 protein following shRNA expression was confirmed by western blot analysis (Fig. 2C). Differential expression analysis showed no off-target gene regulation for any of the three RAD17-targeting shRNA constructs.

RAD17 was validated in the pancreatic cancer cell lines BxPC-3 and MiaPaca-2 as well as the primary cell line JoPaca-1

Table 1. GO annotation cluster enrichment analysis

GO term	P-value	Fold enrichment
GO:0006260~DNA replication	5.83E-04	6.61
GO:0006974~response to DNA damage stimulus	7.29E-03	3.47
GO:0006259~DNA metabolic process	7.62E-03	3.08
GO:0006281~DNA repair	8.09E-03	3.91
GO:0042770~DNA damage response, signal transduction	1.03E-02	8.73
GO:0000077~DNA damage checkpoint	2.60E-02	11.74
GO:0007093~mitotic cell cycle checkpoint	2.89E-02	11.09
GO:0046683~response to organophosphorus	2.93E-02	66.55
GO:0031570~DNA integrity checkpoint	3.04E-02	10.79
GO:0007242~intracellular signalling cascade	4.08E-02	1.78
GO:0045580~regulation of T cell differentiation	4.53E-02	8.68

Genes identified with significant SL effects were used to perform GO annotation cluster enrichment analysis. Significantly enriched GO terms are shown with their respective *P*-values and fold enrichment scores.

(Fredebohm et al., 2012) using increasing concentrations of gemcitabine and *CHK1* knockdown as a positive control. In all three cell lines, knockdown of *RAD17* enhanced gemcitabine cytotoxicity significantly for the three independent shRNA expression constructs. Increased cytotoxicity was most pronounced for 6, 8 and 10 nM gemcitabine. The strongest synthetic lethal effect upon depletion of RAD17 was shown in MiaPaca-2 cells, in which cell viability was reduced from 80% to 20% when treated with 10 nM gemcitabine (Fig. 3). E6/E7-immortalized pancreatic ductal epithelial cells (HPDE) were also susceptible to synthetic lethality.

RAD17 knockdown leads to forced mitotic entry

RAD17 plays a key role in the ATR–CHK1 pathway that is involved in response to stalled replication forks. Knockdown of *RAD17* and *CHK1*, respectively, leads to a clear reduction of cells arrested in early S phase by 50 nM gemcitabine for 24 hours (Fig. 4). To follow up on this population and to determine the cause of increased cytotoxicity, we quantified mitotic cells after knockdown of *RAD17* and *CHK1* with and without gemcitabine using phosphorylated histone 3 (pH3) as a mitotic marker (Hans and Dimitrov, 2001). Knockdown of *RAD17* in combination with 50 nM gemcitabine for 24 hours led to a shift of the mitotic fraction from a tetraploidic (4N) to a less than tetraploidic DNA content (<4N), which was also observed in the CHK1-positive control (Fig. 5). To a lesser extent, this shift was observed for cells in which CHK1 was depleted but that were not treated with gemcitabine. Quantification of this effect revealed that 20–30% of mitotic cells had been forced into mitosis without a fully duplicated genome. Additionally, the sub-G1 fraction of dead cells and debris was increased for cells treated with gemcitabine and depleted of CHK1 or RAD17. Depletion of CHK1 without treatment also resulted in an increase in sub-G1 fraction, more so than depletion of RAD17 (Fig. 5).

Forced mitotic entry is characterized by asymmetric mitosis

Gemcitabine-resistant JoPaca-1 cells were depleted of RAD17 or CHK1, treated with 0.5 and 1 μM gemcitabine for 24 hours and stained for pH3. Cells actively undergoing mitosis were selected and representative images recorded. Although *RAD17* knockdown had little to no effect on normal mitosis, in cells forced into mitosis by a combination of *RAD17* knockdown and gemcitabine anaphase was typically asymmetric (Fig. 6). An increase in gemcitabine concentration led to DNA fragmentation and dispersion following mitotic catastrophe. This phenotype was abundantly observed in gemcitabine-treated MiaPaca-2 cells depleted of RAD17 (Table 2). Analogous to increased sub-G1 fractions we observed an increase in apoptotic cells (Fig. 7). Interestingly, *CHK1* knockdown by itself led to an abnormal amount of JoPaca-1 cells with condensed DNA but no meta- or anaphase phenotypes.

Discussion

In this study, we identified knockdown of *RAD17* as a potentiating factor of gemcitabine-induced cytotoxicity in pancreatic cancer cells. By means of pooled shRNA screening, over 10,000 genes were tested for synthetic lethality with gemcitabine, the standard chemotherapeutic drug used for treatment of advanced pancreatic cancer (Wang et al., 2011). The screen revealed knockdown of 70 genes with significant synthetic lethal effects in combination with gemcitabine. GO annotation cluster enrichment analysis showed a significant enrichment in DNA damage response and repair pathways. Considering the known DNA damaging effect of gemcitabine, this confirmed our methodological approach and the screening conditions applied. More specifically, the ATR–CHK1 pathway known to be directly involved in response to gemcitabine-induced stalled replication forks was clearly overrepresented. An individual validation confirmed strong synthetic lethality of gemcitabine and knockdown of *RAD17* and *CHK1*. In particular, the successful validation of *RAD17* in the primary cell line JoPaca-1 underlines the relevance of this finding, as the cells show a strong resemblance to their primary tumour origin (Fredebohm et al., 2012). Validation of *RAD17* knockdown using three independent shRNA expression constructs minimizes the chance of any off-target effects being responsible for the observed phenotypes (Echeverri et al., 2006). A genome-wide differential expression analysis of mRNA extracts from RAD17-depleted cells and non-silencing controls showed no aberrant gene regulation.

Further characterization of the synergistic effect pointed to forced mitotic entry as the cause of increased cytotoxicity. This has been shown for inhibition of CHK1 and WEE1 (Aarts et al., 2012), and was shown here for RAD17. Immunofluorescence analysis of cells that are forced into mitosis shows a characteristic phenotype of mitotic catastrophe. Although RAD17 depletion without gemcitabine treatment did not result in abnormal mitosis, depletion of CHK1 resulted in premature DNA condensation. Similarly, DNA segregation has been observed in *Chk1*$^{-/-}$

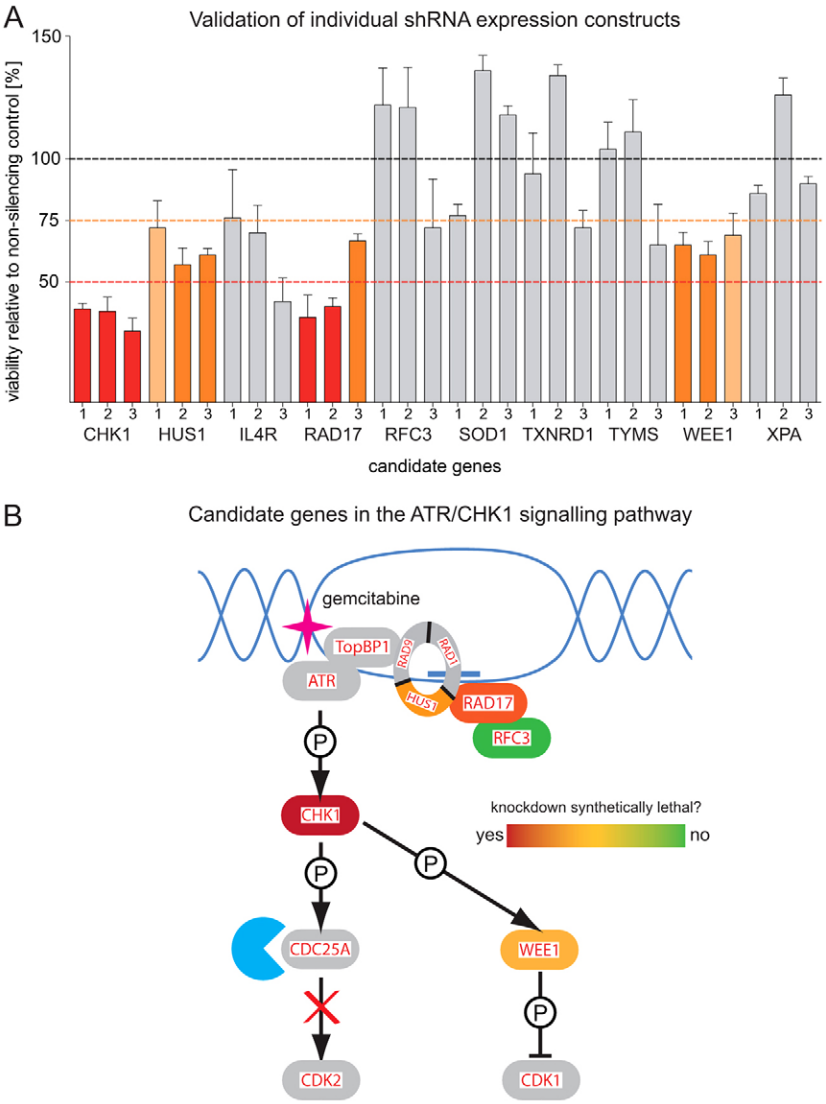

Fig. 2. Validation of candidates. (**A**) Candidate genes were validated in BxPC-3 using three independent shRNA expression constructs. Shown here is the relative viability of treated versus untreated samples. All experiments were done in triplicate. (**B**) Schematic representation of the interactions of important proteins involved in the ATR–CHK1 pathway. Proteins shown in colour were included in the validation experiments. Red to green labelling indicates the intensity of their synthetic lethality effect with gemcitabine upon knockdown (from strong to non-existent). (**C**) Depletion of RAD17 and CHK1 protein was confirmed in BxPC-3, MiaPaca-2 and JoPaca-1 cells by western blot analysis. β-Actin was used as a loading control. Images were subjected to auto-levelling and contrast enhancement.

knockout mice as well, where it results in embryonic death (Takai et al., 2000). The amount of dead cells in the sub-G1 fraction confirms these results and points to increased lethality for *CHK1*-knockdown compared to *RAD17*-knockdown. Cell death following mitotic catastrophe has been suggested to be connected to apoptosis mediated by activation of caspase 2 (Castedo et al., 2004). Although apoptotic cells were higher in mitotically enriched cells undergoing mitotic catastrophe, we could not detect increased caspase-2 activity (data not shown).

Replication fork stalling is a direct result of masked chain termination caused by the incorporation of gemcitabine triphosphate into the nascent DNA strand. This arrest in DNA synthesis needs to be resolved for the cell to replicate its genome and faithfully continue into G2 phase for preparation of mitosis. However, proofreading exonucleases cannot remove the incorporated gemcitabine monophosphate because of its penultimate position (Huang et al., 1991). Moreover, this damage cannot be repaired by any known DNA repair mechanisms: base excision repair, nucleotide excision repair, homologous recombination or non-homologous end joining work (Crul et al., 2003). RAD17 is involved in early events following masked chain termination and replication fork stalling that

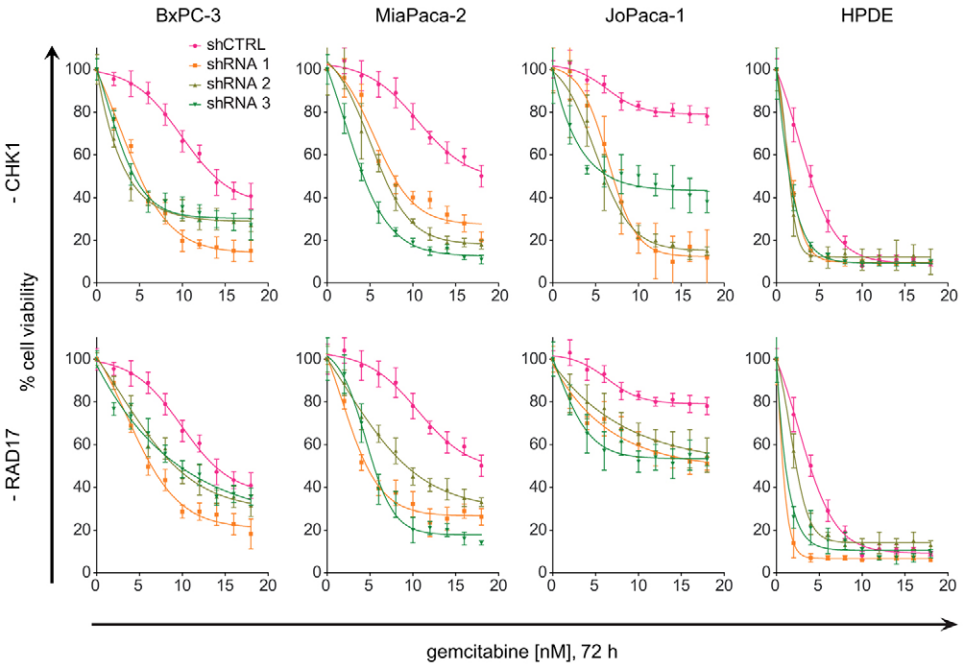

Fig. 3. Validation of RAD17 in cell lines BxPC-3, MiaPaca-2 and JoPaca-1. Knockdown of *RAD17* and *CHK1* with three different shRNA expression constructs each led to increased sensitivity towards gemcitabine. 72 hours after infection, cells were subjected to various concentrations of gemcitabine for another 72 hours. Cell viability was measured by resazurine assay and normalised to the non-treated control.

ultimately lead to intra-S phase arrest through the ATR–CHK1 pathway. The first step in recognition of the stalled fork is the recruitment of ataxia telangiectasia and Rad3-related protein (ATR) by binding of its close partner ATR-interacting protein (ATRIP) to replication protein A (RPA) bound to exposed single-strand DNA (Cortez et al., 2001; Zou and Elledge, 2003). The second step of activating the ATR–CHK1 signalling cascade starts with the recruitment of polymerase α (Pol α) to the leading strand by topoisomerase-2 binding protein 1 (TopBP1), which also binds to RPA (Yan and Michael, 2009). Pol α then creates primer-template junctions on the leading strand and mediates recruitment of the heterotrimeric DNA clamp complex of RAD9–HUS1–RAD1 (9-1-1) (Yan and Michael, 2009). In order to form a ring around the DNA, the 9-1-1 clamp needs to be loaded. This is mediated by a complex consisting of RAD17 and the small subunits of replication factor C (RFC2-5) called the clamp loader complex (Lee and Dunphy, 2010; Shiomi et al., 2002). The clamp loader complex binds to RPA-coated single-strand DNA at the 5′-end of a primer template junction where it loads the 9-1-1 clamp onto the DNA (Majka et al., 2006). In order to activate ATR and downstream effector kinases such as CHK1, cooperation between RAD17/RFC2-5, 9-1-1 and TopBP1 is important. Furthermore, RAD17 function is a prerequisite for this connection, as it is required for the interaction between TopBP1

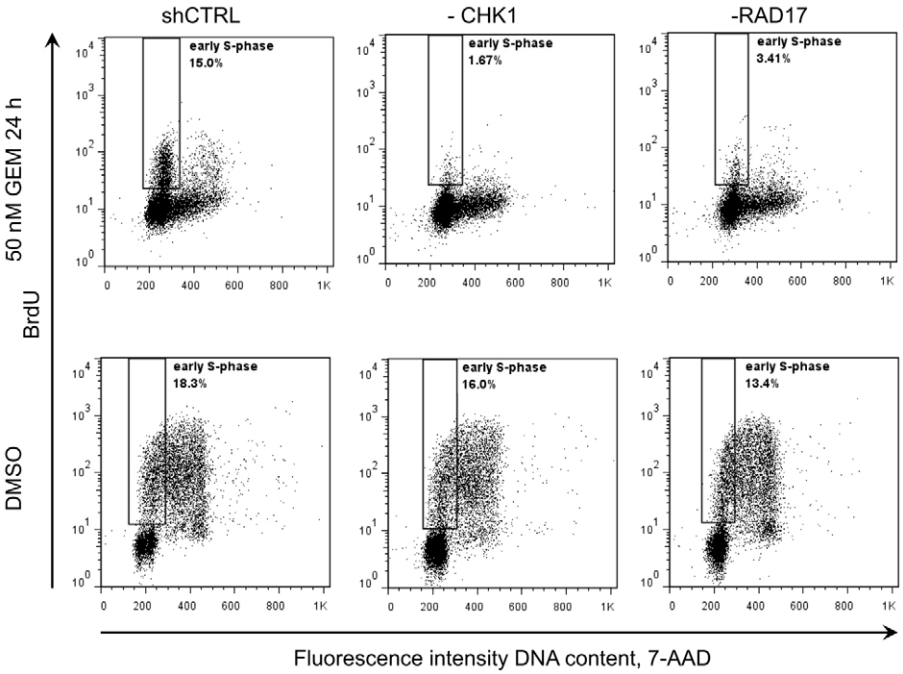

Fig. 4. Depletion of cells arrested in early S phase. Long-term BrdU incorporation following gemcitabine treatment shows cell cycle arrest in early S phase in BxPC-3 cells treated with non-silencing control. Knockdown of CHK1 and RAD17 leads to depletion of this population.

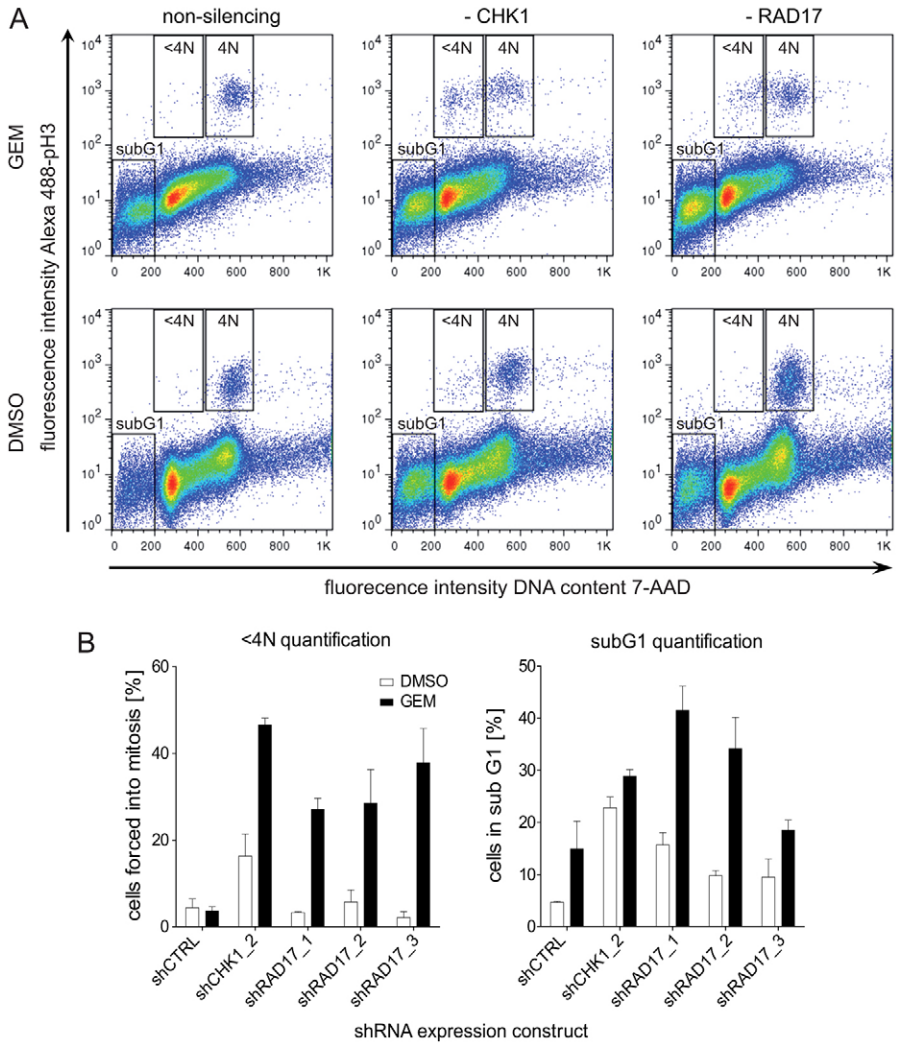

Fig. 5. Forced mitotic entry and sub-G1 increase. Knockdown of *RAD17* and *CHK1* led to forced mitotic entry of cells that were arrested in S phase by a gemcitabine treatment of 50 nM for 24 hours. (**A**) Fluorescence activated cell sorting (FACS) profiles showed an increase in mitotic cells (pH3-positive) without fully duplicated genomes (<4N) after knockdown of *RAD17* and *CHK1*, when treated with gemcitabine. (**B**) Cells forced into mitosis (<4N) were counted and are shown as a percentage of all mitotic cells. Cells in sub-G1 were counted as well, and expressed as a percentage of all cells.

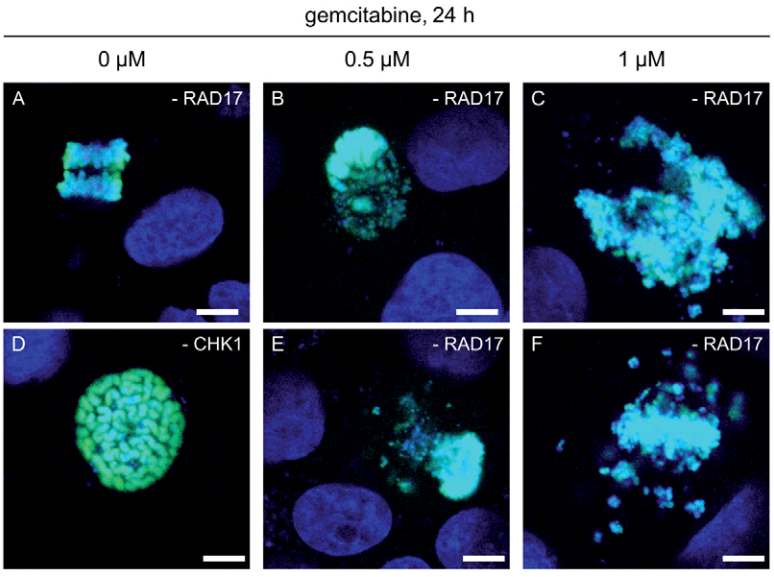

Fig. 6. Asymmetric mitosis, DNA fragmentation and mitotic catastrophe. Knockdown of *RAD17* followed by gemcitabine treatment led to asymmetric mitosis and DNA fragmentation. Shown here are merged images of pH3-positive cells during or after asymmetric mitosis. Normal mitosis was observed for *RAD17*-knockdown cells without gemcitabine (**A**), but cells forced into mitosis without duplicated genomes underwent asymmetric mitosis (**B**,**E**) and fragmentation of DNA (**C**,**F**). Knockdown of *CHK1* led to an abnormal number of cells showing DNA condensation without meta- or anaphase phenotypes (**D**). Scale bars: 10 µm.

Table 2. Quantification of asymmetric mitosis

		pH3-positive cells	
	nM GEM	Normal anaphase	Asymmetric mitosis
shCTRL	0	60	1
shCTRL	50	30	1
shRAD17	0	46	2
shRAD17	50	9	42

Asymmetric mitosis of MiaPaca-2 cells treated with shRAD17 and shCTRL with or without 50 nM gemcitabine was quantified microscopically. Numbers are actual cell counts.

and RAD9 and for increased recruitment of TopBP1 to the stalled replication fork (Lee and Dunphy, 2010).

This pathway not only regulates arrest during S phase upon DNA damage, but also affects the G2–M transition through its key regulator CHK1. Triggering activation of CHK1 engages two powerful mechanisms influencing cell-cycle regulation. Firstly, active CHK1 causes intra-S phase arrest by degradation of CDC25A phosphatase, which is responsible for activation of CDK2-cyclin A/E complexes (Boutros et al., 2007). Secondly, it inhibits G2–M transition by activation of WEE1, which is responsible for inhibition of CDK1/cyclin B complex (Boutros et al., 2007; O'Connell et al., 1997). Thus, early inhibition of this pathway results in cessation of cell cycle arrest and procession into premature mitosis.

Our results underline the importance of RAD17 in this mechanism. Also, they suggest RAD17 as a new target for gemcitabine combination therapy. Targeting the ATR–CHK1 pathway has become a promising approach for pancreatic cancer and other cancer entities (Carrassa and Damia, 2011; Garrett and Collins, 2011). Inhibitors of CHK1 are currently under clinical investigation [comprehensively reviewed by Garrett and Collins (Garrett and Collins, 2011)]. Similarly, a potent inhibitor of WEE1 kinase (MK-1775) shows promising results in preclinical experiments and is now included in phase I clinical studies with gemcitabine and platinum-based drugs. Combination of CHK1 and WEE1 inhibition has shown synergistic cytotoxicity (Aarts et al., 2012; Davies et al., 2011) illustrating the promising potential of targeting this pathway. Along this line, development of RAD17 inhibitors should provide a new option for combination with gemcitabine as well as CHK1 and WEE1 inhibitors.

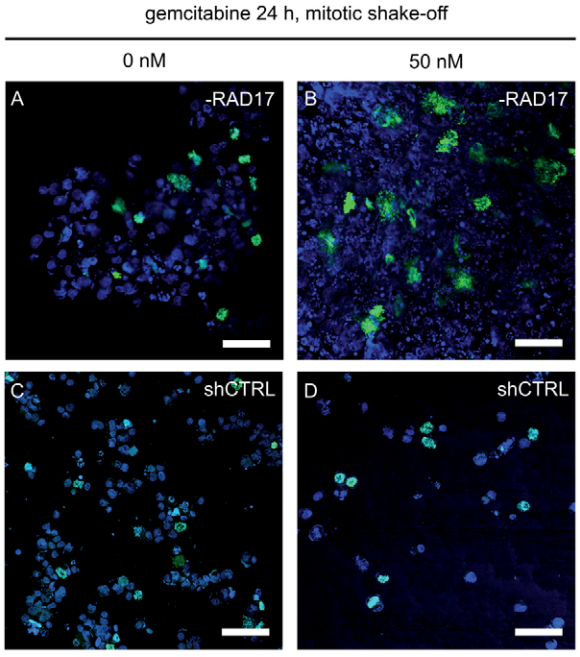

Fig. 7. Quantification of asymmetric mitosis. Asymmetric mitosis was quantified microscopically in mitotically enriched MiaPaca-2 cells depleted of RAD17 (**A**,**B**) with or without 50 nM gemcitabine for 24 hours compared to the non-silencing control (shCTRL; **C**,**D**). The synthetic lethal effect leads to an increase in DNA fragmentation and dispersion in pH3-positive cells (green; B). Scale bars: 100 μm.

The synthetic lethal effect of CHK1 and WEE1 inhibition in combination with DNA-damaging agents has been shown to be dependent on p53 deficiency (Aarts et al., 2012; Chen et al., 2006; Landau et al., 2012; Ma et al., 2012). The tumour suppressor protein p53 is a key regulator of cell-cycle arrest in response to DNA damage. Upon activation, it acts as a transcription factor of CDK inhibitors such as p21 (*CDKN1A*) and p16 (*CDKN2A*) (Alberts, 2002). Through this route, functional p53 signalling may override unscheduled mitotic entry triggered by inhibition of the ATR–CHK1 signalling pathway. Concordantly, E6/E7-immortalized HPDE cells with defective p53 signalling (Ouyang et al., 2000) were susceptible to synthetic lethality of *CHK1* or *RAD17* knockdown in combination with gemcitabine. BxPC-3 and MiaPaca-2 cell lines both carry deleterious mutations in the DNA-binding domain of p53 (Petitjean et al., 2007) necessary for transcriptional regulation. JoPaca-1 cells, however, have a mutation solely at codon 72 of the proline-rich domain that is important for induction of apoptosis but not cell-cycle arrest (Baptiste et al., 2002; Fredebohm et al., 2012; Walker and Levine, 1996; Zhu et al., 1999). However, the functional DNA-binding domain of p53 in JoPaca-1 cells does not prevent sensitivity to the synthetic lethality of CHK1 and RAD17 inhibition and gemcitabine.

Nevertheless, the lack of mutations in the DNA-binding domain of p53 in JoPaca-1cells may account for the slightly reduced synthetic lethal effect compared with that in BxPC-3 and MiaPaca-2 cells. Future studies will have to determine which mutations are most sensitive in the functional dependence of CHK1–ATR pathway inhibition on p53-regulated cell-cycle arrest. Once this is clarified, clinical application of CHK1/WEE1, and potentially RAD17 inhibitors, should be accompanied by molecular diagnostics of patient p53-mutational status.

As shown here and elsewhere (Azorsa et al., 2009), knockdown of CHK1 has a proliferation inhibiting effect on its own, characterized by abnormal chromosomal segregation. Therefore, inhibition of CHK1 is likely to cause undesired cytotoxicity in normal cells causing increased side effects. RAD17 knockdown by itself did not inhibit cell proliferation nor did it show abnormal DNA segregation. Given the central role of CHK1 in many DNA-damage response pathways (Carrassa and Damia, 2011), targeting the replication fork stalling pathway at the position of RAD17, upstream of CHK1 and WEE1, might provide a more specific approach.

Materials and Methods

Cell culture

The pancreatic cancer cell lines MiaPaCa-2 and BxPC-3 were obtained from ATCC (Rockville, MD, USA). The primary cell line JoPaca-1 was isolated as described previously (Fredebohm et al., 2012) and used at low passage (<P10) to retain primary characteristics. HPDE cells were kindly provided by Professor

Francisco Real (Spanish National Cancer Research Centre, CNIO). All cell lines were free of mycoplasms, viruses and cell line contamination as tested by PCR (Schmitt and Pawlita, 2009). Cells were cultured in standard medium and supplements, which were obtained from Life Technologies, Darmstadt, Germany: BxPC-3 in Roswell Park Memorial Institute (RPMI) 1640 medium (cat. no. 21875), MiaPaCa-2 in Dulbecco's modified Eagle's medium (DMEM; cat. no. 41965) supplemented with 1 mM sodium pyruvate (cat. no. 11360), and JoPaca-1 in Isocove's modified Dulbecco's medium (IMDM; cat. no. 21056); HPDE in keratinocyte serum-free medium (KSFM), 0.15 ng/ml epidermal growth factor receptor and 25 µg/ml bovine pituitary extract (cat. no. 17005075). All media were supplemented with 10% foetal calf serum (cat. no. 10500) and 1% penicillin–streptomycin (cat. no. 15140).

Screening conditions

We targeted 10,000 genes for shRNA-mediated knockdown using modules 1 and 2 of the Decipher library (Cellecta, Mountain View, CA, USA) in two screens under identical conditions. Each gene was targeted by five shRNA expression constructs, which are identifiable by barcode sequences. The target cell line BxPC-3 was infected with lentiviral particles containing either module 1 or 2 at a multiplicity of infection of 0.3. Positively infected cells were selected by addition of 0.5 µg/ml puromycin 24 hours after infection. Selection took place for 48 hours, after which puromycin was removed and cells were allowed to recover for another 48 hours. After recovery, cells were divided into treatment and control groups. At this point, a sample of 20 million cells was taken for the t_0 reference time point, shock-frozen and kept at −80℃. Cells were kept under selective pressure of 0.5 µg/ml puromycin, which was added after cells had attached to the substrate. A 72-hour treatment with 6 nM gemcitabine, or DMSO as a control, commenced 48 hours after passaging. After an additional 72 hours without treatment, control and treated cells were harvested, shock-frozen and kept at −80℃.

Barcode amplification

To determine the abundance of cells before and after treatment and in the DMSO control, barcode sequences were amplified from genomic DNA and subjected to high-throughput sequencing. Amplification of barcode sequences was achieved by two rounds of PCR according to the following protocol. Cell pellets from samples obtained at the t_0, $t_{\text{end-GEM}}$ and $t_{\text{end-CTRL}}$ time points were thawed and subjected to ultrasonication at 50% intensity for 10 seconds on ice to shear genomic DNA into fragments of 1–10 kb. Genomic DNA was isolated from cell pellets using DNeasy Blood & Tissue Kit (69581, Qiagen, Hilden, Germany). For the first round of PCR, 50 µg of fragmented genomic DNA were used in eight 100 µl reactions containing: 1 µl Titantium Taq polymerase and corresponding PCR buffer (639210, Clontech of Takara Bio, Saint-Germain-en-Laye, France), 250 µM dNTP mix (M3015.4100, Genaxxon, Ulm, Germany), 3 µM HTS forward primer: 5′-TTCTCTGGCAAGCAAAAGACGGCATA-3′ and 3 µM reverse primer: 5′-TGCCATTTGTCTCGAGGTCGAGAA-3′ in nuclease-free water (AM9938, Life Technologies, Darmstadt, Germany). Desalted purity primers were obtained from Sigma Aldrich (Munich, Germany). Reaction mixtures were prepared on ice and subjected to a first round PCR starting with activation of the polymerase at 94℃ for 3 minutes, followed by 16 cycles of denaturation at 94℃ for 30 seconds, annealing at 65℃ for 10 seconds, and elongation at 72℃ for 20 seconds. Final extension was done at 68℃ for 2 minutes. Second round PCR was done using 2 µl of the first-round reaction as template in three 100 µl reactions per condition. This time, primers GEX forward 5′-CAAGCAGAAGACGGCATACGAGA-3′ and GEX reverse 5′-AATGATACGGCGACCACCGAGA-3′ were used, while all other reagents remained the same. Thermal cycler settings were also unchanged, with the exception of a reduced elongation time of 10 seconds and a reduction of the cycle number to ten. Amplified barcode sequences were purified using PCR purification and gel extraction kits (28104 and 28704, Qiagen). Barcodes of module 1 and 2 were combined for each time point and quantified by next-generation sequencing (Genome Analyzer IIx, Illumina, San Diego, CA, USA). Each module contained a two-base-pair identifier attached to the barcode sequence for later discrimination.

Sequencing data analysis

Sequences were analysed to determine the abundance of each barcode using the software 'Barcode Deconvoluter' provided by Cellecta. The software counts the number of 18-nucleotide barcode sequences with a tolerance of two mismatches and assigns each barcode to the corresponding shRNA construct. Furthermore, each module was identified by two module-specific base pairs attached to the barcode sequence. Further analysis was done in Microsoft Excel. In order to compare reads of different modules and time points, each group of modules and time points was normalized to the average number of reads. Barcodes below 100 reads for t_0 and $t_{\text{end-CTRL}}$ were filtered out for reasons of quality assurance. Finally, SL ratios were calculated by dividing normalised reads of $t_{\text{end-GEM}}$ by normalised reads of $t_{\text{end-CTRL}}$ and taking the $\log_2$ of this ratio. Genes passing these filter criteria with at least three shRNA expression constructs were averaged and a *P*-value calculated in comparison to internal luciferase control constructs using unpaired, two-sided, unequal variance *t*-test statistics. Candidates for further analysis were selected on the basis of the strength and significance of the SL ratio. Following this principle, genes were included when significance was below a *P*-value of 0.05 and the $\log_2$ SL ratio was below −0.35. Selection of candidates for validation was assisted by functional annotation enrichment analysis (Huang et al., 2009).

Production of lentiviral particles

Lentiviral particles were produced using a second generation system described and engineered by Didier Trono's group (Zufferey et al., 1997). HEK-293T cells were seeded in DMEM without antibiotics at a density of 65,000 cells per cm^2 in a six-well format for single constructs or 175 cm^2 flasks for production of viral pools. Helper plasmids psPAX2 and pMD2.G were co-transfected with the construct carrier pRSI9 the following day using Lipofectamine (18324010, Life Technologies) and Plus Reagent (11514015, Life Technologies) according to the manufacturer's instructions. The next day, the medium was exchanged for high-serum DMEM (30% FCS). Supernatant containing lentiviral particles was harvested the following day, filtered through a 0.45 µm PES membrane (295–4545, Thermo Scientific) and stored in aliquots at −80℃.

Individual validation procedure

For each candidate gene, three shRNA expression constructs were cloned into pRSI9-U6-(sh)-UbiC-TagRFP-2A-Puro vector according to the supplier's protocols and validated by Sanger sequencing. All shRNA sequences used for candidate validation are listed in supplementary material Table S3. Lentivirus was produced and titrated for each cell line to yield an optimal dilution factor for multiplicity of infection between 1 and 2 for 24 hours of infection. In a first round of validation, BxPC-3 was treated 72 hours after infection with 6 nM gemcitabine for 72 hours. Cell viability, determined by the resazurine assay (Czekanska, 2011), was normalised to the non-silencing control (shCTRL) for treatment and control conditions, respectively, and expressed in percentages. shRNAs against *RAD17* and *CHK1* were further validated in MiaPaca-2 cells and the primary cell line JoPaca-1 using concentrations of gemcitabine between 0 and 18 nM.

Expression profiling

Total RNA was isolated with the RNAeasy Isolation kit (Qiagen, Hilden, Germany), following the protocol suggested by the manufacturer. RNA integrity was evaluated using an Agilent 2100 Bioanalyzer (Agilent Technologies, Palo Alto, USA). The RNA was analysed on the HumanHT-12 v4 Whole Genome Expression BeadChip (Illumina, San Diego, CA). To synthesize first and second strand cDNA and for amplifying biotinylated cRNA, the Illumina Totalprep RNA Amplification Kit was used. Hybridisation to the BeadChip was performed according to the manufacturer's instructions without modification. In short, a maximum of 10 µl cRNA was mixed with a 20 µl GEX-HYB hybridisation solution. The preheated 30 µl assay sample was dispensed onto the large sample port of each array and incubated for 18 hours at 58℃. Subsequently, the samples were washed and scanned with a BeadArray Reader (Illumina). Raw data were exported from the Illumina Beadstudio software to R (Ritchie et al., 2011). The data were quantile normalised and $\log_2$ transformed. The expression data are available in the ArrayExpress database (http://www.ebi.ac.uk/arrayexpress) under accession number E-MTAB-1535.

Western blot and fluorescence activated cell sorting

Infected and selected cells were lysed in M-PER lysis buffer (78501, Pierce, Thermo Scientific) containing complete protease inhibitors (04719964001, Roche, Mannheim, Germany) 1 tablet per 10 ml, 1 mM NaF and 0.2 µM Na_3VO_4. SDS-PAGE and western blotting were done according to standard protocols (Sambrook and Russell, 2006). The following primary antibodies were used for validation of gene knockdown: mouse Chk1 (G-4; sc-8408, Santa Cruz, Heidelberg, Germany); rabbit Rad17 D3G6 (8561, Cell Signaling Technology, Frankfurt, Germany) and for loading control, antibodies against β-actin (rabbit polyclonal, ab8227, Abcam, Cambridge, UK and mouse monoclonal, A5316, Sigma Aldrich, Taufkirchen, Germany). Western blots were incubated with ECL plus (32132, Thermo Scientific) and exposed using a chemiluminescent image analyzer (LAS-4000 mini, Fuji Film, Düsseldorf, Germany). Images were improved in Photoshop-CS5 (Adobe Systems GmbH, Munich, Germany) using auto-level functions for tone and contrast enhancement. Phospho-histone-3-positive cells were quantified by fluorescence activated cell sorting (FACS; Canto II, BD Biosciences, Heidelberg, Germany) after fixation in 70% ethanol and permeabilisation with 0.25% Triton X-100 using phospho-histone H3 (Ser10) antibody conjugated to Alexa-Fluor-488 (3465, Cell Signaling Technology). DNA was counterstained with 7-amino-actinomycin D (7-AAD; cat. no. 559925, BD Biosciences). FACS data were acquired using FACSDiva (BD Biosciences) and analysed using FlowJo software (Tree Star, Ashland, OR, USA).

Immunofluorescence

For immunofluorescence of pH3-positive cells, JoPaca-1 cells depleted of RAD17 or CHK1 were grown in culture slides (cat. no. 354559, BD Biosciences) and

treated with 0.5 μM and 1 μM gemcitabine for 24 hours. Cells were fixed with 3.7% formaldehyde and permeabilised with 0.25% Triton X-100. Slides were incubated with the same Alexa-Fluor-488 pH3 antibody used in FACS experiments for 18 hours at 4℃. After removing the chambers coverslips were fixed on top of the slides by Vectashield® mounting medium containing 4′,6-diamidin-2-phenylindol (DAPI) to counter-stain nuclei (H-1500, Vector Laboratories, Burlingame, CA, USA). Images were taken with a confocal laser scanning microscope (LSM 700, Carl Zeiss Microscopy, Oberkochen, Germany).

Quantification of asymmetric mitosis was done using MiaPaca-2 cells depleted of RAD17 with or without 50 nM gemcitabine, compared with cells treated with shCTRL. Mitotic cells were enriched by mitotic shake-off at 250 r.p.m. for 30 minutes and collected with dead cells in the supernatant. Cells were fixed, permeabilised and stained for pH3 as described above. For quantification, five to ten images were taken at random locations on the slide.

Acknowledgements

The authors thank Philipp Kuhn, Sandra Widder and Viola Ladenburger for technical assistance. Lentiviral shRNA libraries were kindly provided and developed by Cellecta using National Institutes of Health funded research grant support.

Author contributions

J.F.: study concept and design; acquisition of data; analysis and interpretation of data; drafting of the manuscript. J.W.: technical and material support; acquisition of data; data analysis. J.D.H.: study concept and design; interpretation of data; drafting of the manuscript; obtained funding; study supervision. M.B.: study concept and design; acquisition of data; analysis and interpretation of data; study supervision.

Funding

This work was supported by the German Federal Ministry of Education and Research (BMBF) as part of the NGFN PaCaNet project [grant number 01GS08117 to J.D.H.].

Supplementary material available online at
http://jcs.biologists.org/lookup/suppl/doi:10.1242/jcs.124768/-/DC1

References

Aarts, M., Sharpe, R., Garcia-Murillas, I., Gevensleben, H., Hurd, M. S., Shumway, S. D., Toniatti, C., Ashworth, A. and Turner, N. C. (2012). Forced mitotic entry of S-phase cells as a therapeutic strategy induced by inhibition of WEE1. *Cancer Discov.* **2**, 524-539.

Alberts, B. (2002). *Molecular Biology of the Cell*. New York, NY: Garland Science.

Azorsa, D. O., Gonzales, I. M., Basu, G. D., Choudhary, A., Arora, S., Bisanz, K. M., Kiefer, J. A., Henderson, M. C., Trent, J. M., Von Hoff, D. D. et al. (2009). Synthetic lethal RNAi screening identifies sensitizing targets for gemcitabine therapy in pancreatic cancer. *J. Transl. Med.* **7**, 43.

Baptiste, N., Friedlander, P., Chen, X. and Prives, C. (2002). The proline-rich domain of p53 is required for cooperation with anti-neoplastic agents to promote apoptosis of tumor cells. *Oncogene* **21**, 9-21.

Boutros, R., Lobjois, V. and Ducommun, B. (2007). CDC25 phosphatases in cancer cells: key players? Good targets? *Nat. Rev. Cancer* **7**, 495-507.

Carrassa, L. and Damia, G. (2011). Unleashing Chk1 in cancer therapy. *Cell Cycle* **10**, 2121-2128.

Castedo, M., Perfettini, J. L., Roumier, T., Valent, A., Raslova, H., Yakushijin, K., Horne, D., Feunteun, J., Lenoir, G., Medema, R. et al. (2004). Mitotic catastrophe constitutes a special case of apoptosis whose suppression entails aneuploidy. *Oncogene* **23**, 4362-4370.

Chen, Z., Xiao, Z., Gu, W. Z., Xue, J., Bui, M. H., Kovar, P., Li, G., Wang, G., Tao, Z. F., Tong, Y. et al. (2006). Selective Chk1 inhibitors differentially sensitize p53-deficient cancer cells to cancer therapeutics. *Int. J. Cancer* **119**, 2784-2794.

Cortez, D., Guntuku, S., Qin, J. and Elledge, S. J. (2001). ATR and ATRIP: partners in checkpoint signaling. *Science* **294**, 1713-1716.

Crul, M., van Waardenburg, R. C., Bocxe, S., van Eijndhoven, M. A., Pluim, D., Beijnen, J. H. and Schellens, J. H. (2003). DNA repair mechanisms involved in gemcitabine cytotoxicity and in the interaction between gemcitabine and cisplatin. *Biochem. Pharmacol.* **65**, 275-282.

Czekanska, E. M. (2011). Assessment of cell proliferation with resazurin-based fluorescent dye. *Methods Mol. Biol.* **740**, 27-32.

Davies, K. D., Cable, P. L., Garrus, J. E., Sullivan, F. X., von Carlowitz, I., Huerou, Y. L., Wallace, E., Woessner, R. D. and Gross, S. (2011). Chk1 inhibition and Wee1 inhibition combine synergistically to impede cellular proliferation. *Cancer Biol. Ther.* **12**, 788-796.

Echeverri, C. J., Beachy, P. A., Baum, B., Boutros, M., Buchholz, F., Chanda, S. K., Downward, J., Ellenberg, J., Fraser, A. G., Hacohen, N. et al. (2006). Minimizing the risk of reporting false positives in large-scale RNAi screens. *Nat. Methods* **3**, 777-779.

Fredebohm, J., Boettcher, M., Eisen, C., Gaida, M. M., Heller, A., Keleg, S., Tost, J., Greulich-Bode, K. M., Hotz-Wagenblatt, A., Lathrop, M. et al. (2012). Establishment and characterization of a highly tumourigenic and cancer stem cell enriched pancreatic cancer cell line as a well defined model system. *PLoS ONE* **7**, e48503.

Garrett, M. D. and Collins, I. (2011). Anticancer therapy with checkpoint inhibitors: what, where and when? *Trends Pharmacol. Sci.* **32**, 308-316.

Glienke, W., Maute, L., Wicht, J. and Bergmann, L. (2012). The dual PI3K/mTOR inhibitor NVP-BGT226 induces cell cycle arrest and regulates Survivin gene expression in human pancreatic cancer cell lines. *Tumour Biol.* **33**, 757-765.

Hackert, T., Büchler, M. W. and Werner, J. (2009). Surgical options in the management of pancreatic cancer. *Minerva Chir.* **64**, 465-476.

Hans, F. and Dimitrov, S. (2001). Histone H3 phosphorylation and cell division. *Oncogene* **20**, 3021-3027.

Heinemann, V., Boeck, S., Hinke, A., Labianca, R. and Louvet, C. (2008). Meta-analysis of randomized trials: evaluation of benefit from gemcitabine-based combination chemotherapy applied in advanced pancreatic cancer. *BMC Cancer* **8**, 82.

Huang, P., Chubb, S., Hertel, L. W., Grindey, G. B. and Plunkett, W. (1991). Action of 2′,2′-difluorodeoxycytidine on DNA synthesis. *Cancer Res.* **51**, 6110-6117.

Huang, D. W., Sherman, B. T. and Lempicki, R. A. (2009). Bioinformatics enrichment tools: paths toward the comprehensive functional analysis of large gene lists. *Nucleic Acids Res.* **37**, 1-13.

Hung, S. W., Mody, H. R. and Govindarajan, R. (2012). Overcoming nucleoside analog chemoresistance of pancreatic cancer: a therapeutic challenge. *Cancer Lett.* **320**, 138-149.

Iorns, E., Lord, C. J., Turner, N. and Ashworth, A. (2007). Utilizing RNA interference to enhance cancer drug discovery. *Nat. Rev. Drug Discov.* **6**, 556-568.

Kassner, P. D. (2008). Discovery of novel targets with high throughput RNA interference screening. *Comb. Chem. High Throughput Screen.* **11**, 175-184.

Kern, S. E., Shi, C. and Hruban, R. H. (2011). The complexity of pancreatic ductal cancers and multidimensional strategies for therapeutic targeting. *J. Pathol.* **223**, 295-306.

Ko, A. H., Youssoufian, H., Gurtler, J., Dicke, K., Kayaleh, O., Lenz, H. J., Keaton, M., Katz, T., Ballal, S. and Rowinsky, E. K. (2012). A phase II randomized study of cetuximab and bevacizumab alone or in combination with gemcitabine as first-line therapy for metastatic pancreatic adenocarcinoma. *Invest. New Drugs* **30**, 1597-1606.

Landau, H. J., McNeely, S. C., Nair, J. S., Comenzo, R. L., Asai, T., Friedman, H., Jhanwar, S. C., Nimer, S. D. and Schwartz, G. K. (2012). The checkpoint kinase inhibitor AZD7762 potentiates chemotherapy-induced apoptosis of p53-mutated multiple myeloma cells. *Mol. Cancer Ther.* **11**, 1781-1788.

Lee, J. and Dunphy, W. G. (2010). Rad17 plays a central role in establishment of the interaction between TopBP1 and the Rad9-Hus1-Rad1 complex at stalled replication forks. *Mol. Biol. Cell* **21**, 926-935.

Ma, Z., Yao, G., Zhou, B., Fan, Y., Gao, S. and Feng, X. (2012). The Chk1 inhibitor AZD7762 sensitises p53 mutant breast cancer cells to radiation in vitro and in vivo. *Mol. Med. Rep.* **6**, 897-903.

Majka, J., Binz, S. K., Wold, M. S. and Burgers, P. M. (2006). Replication protein A directs loading of the DNA damage checkpoint clamp to 5′-DNA junctions. *J. Biol. Chem.* **281**, 27855-27861.

Merl, M. Y., Abdelghany, O., Li, J. and Saif, M. W. (2010). First-line treatment of metastatic pancreatic adenocarcinoma: can we do better? Highlights from the "2010 ASCO Annual Meeting". Chicago, IL, USA. June 4-8, 2010. *JOP* **11**, 317-320.

Moore, M. J., Goldstein, D., Hamm, J., Figer, A., Hecht, J. R., Gallinger, S., Au, H. J., Murawa, P., Walde, D., Wolff, R. A. et al.; National Cancer Institute of Canada Clinical Trials Group (2007). Erlotinib plus gemcitabine compared with gemcitabine alone in patients with advanced pancreatic cancer: a phase III trial of the National Cancer Institute of Canada Clinical Trials Group. *J. Clin. Oncol.* **25**, 1960-1966.

O'Connell, M. J., Raleigh, J. M., Verkade, H. M. and Nurse, P. (1997). Chk1 is a wee1 kinase in the G2 DNA damage checkpoint inhibiting cdc2 by Y15 phosphorylation. *EMBO J.* **16**, 545-554.

Ouyang, H., Mou, L., Luk, C., Liu, N., Karaskova, J., Squire, J. and Tsao, M. S. (2000). Immortal human pancreatic duct epithelial cell lines with near normal genotype and phenotype. *Am. J. Pathol.* **157**, 1623-1631.

Petitjean, A., Mathe, E., Kato, S., Ishioka, C., Tavtigian, S. V., Hainaut, P. and Olivier, M. (2007). Impact of mutant p53 functional properties on TP53 mutation patterns and tumor phenotype: lessons from recent developments in the IARC TP53 database. *Hum. Mutat.* **28**, 622-629.

Philip, P. A. (2008). Targeted therapies for pancreatic cancer. *Gastrointest Cancer Res.* **2 Suppl.**, S16-S19.

Ritchie, M. E., Dunning, M. J., Smith, M. L., Shi, W. and Lynch, A. G. (2011). BeadArray expression analysis using bioconductor. *PLoS Comput. Biol.* **7**, e1002276.

Safran, H., Iannitti, D., Ramanathan, R., Schwartz, J. D., Steinhoff, M., Nauman, C., Hesketh, P., Rathore, R., Wolff, R., Tantravahi, U. et al. (2004). Herceptin and gemcitabine for metastatic pancreatic cancers that overexpress HER-2/neu. *Cancer Invest.* **22**, 706-712.

Sambrook, J. and Russell, D. W. (2006). SDS-polyacrylamide gel electrophoresis of proteins. *CSH Protoc* 2006.

Schmitt, M. and Pawlita, M. (2009). High-throughput detection and multiplex identification of cell contaminations. *Nucleic Acids Res.* **37**, e119.

Shiomi, Y., Shinozaki, A., Nakada, D., Sugimoto, K., Usukura, J., Obuse, C. and Tsurimoto, T. (2002). Clamp and clamp loader structures of the human checkpoint protein complexes, Rad9-1-1 and Rad17-RFC. *Genes Cells* **7**, 861-868.

Siegel, R., Naishadham, D. and Jemal, A. (2013). Cancer statistics, 2013. *CA Cancer J. Clin.* **63**, 11-30.

Stathis, A. and Moore, M. J. (2010). Advanced pancreatic carcinoma: current treatment and future challenges. *Nat. Rev. Clin Oncol.* **7**, 163-172.

Takai, H., Tominaga, K., Motoyama, N., Minamishima, Y. A., Nagahama, H., Tsukiyama, T., Ikeda, K., Nakayama, K., Nakanishi, M. and Nakayama, K. (2000). Aberrant cell cycle checkpoint function and early embryonic death in Chk1(-/-) mice. *Genes Dev.* **14**, 1439-1447.

Venkatesha, V. A., Parsels, L. A., Parsels, J. D., Zhao, L., Zabludoff, S. D., Simeone, D. M., Maybaum, J., Lawrence, T. S. and Morgan, M. A. (2012). Sensitization of pancreatic cancer stem cells to gemcitabine by Chk1 inhibition. *Neoplasia* **14**, 519-525.

Walker, K. K. and Levine, A. J. (1996). Identification of a novel p53 functional domain that is necessary for efficient growth suppression. *Proc. Natl. Acad. Sci. USA* **93**, 15335-15340.

Wang, Z., Li, Y., Ahmad, A., Banerjee, S., Azmi, A. S., Kong, D. and Sarkar, F. H. (2011). Pancreatic cancer: understanding and overcoming chemoresistance. *Nat. Rev. Gastroenterol Hepatol.* **8**, 27-33.

Yan, S. and Michael, W. M. (2009). TopBP1 and DNA polymerase alpha-mediated recruitment of the 9-1-1 complex to stalled replication forks: implications for a replication restart-based mechanism for ATR checkpoint activation. *Cell Cycle* **8**, 2877-2884.

Zhu, J., Jiang, J., Zhou, W., Zhu, K. and Chen, X. (1999). Differential regulation of cellular target genes by p53 devoid of the PXXP motifs with impaired apoptotic activity. *Oncogene* **18**, 2149-2155.

Zou, L. and Elledge, S. J. (2003). Sensing DNA damage through ATRIP recognition of RPA-ssDNA complexes. *Science* **300**, 1542-1548.

Zufferey, R., Nagy, D., Mandel, R. J., Naldini, L. and Trono, D. (1997). Multiply attenuated lentiviral vector achieves efficient gene delivery in vivo. *Nat. Biotechnol.* **15**, 871-875.